

Progressive Covering of the Accretion Disk Corona during Dipping in the LMXB XB 1916-053

R. Morley¹, M. J. Church¹, A. P. Smale² and M. Bałucińska-Church¹

¹*School of Physics and Astronomy, University of Birmingham, Birmingham, B15 2TT, UK*

e-mail: rm@star.sr.bham.ac.uk, mjc@star.sr.bham.ac.uk, mbc@star.sr.bham.ac.uk

²*Laboratory for High Energy Astrophysics, Code 660.2, NASA/Goddard Space Flight Center, MD 20771, USA*

e-mail: alan@osiris.gsfc.nasa.gov

Accepted. Received

ABSTRACT

Results are reported for analysis of the extensive *Rosat* observation of the dipping low mass X-ray binary XB 1916-053. Dipping is 100% deep showing that the emission regions are completely covered by the absorber. A good fit to the non-dip spectrum is obtained using a model consisting of a blackbody with $kT_{\text{BB}} = 1.95^{+0.74}_{-0.34}$ keV and a power law with photon index 2.32 ± 0.04 . These components are identified with emission from the neutron star, and Comptonized emission from an extended accretion disk corona (ADC). Dip spectra are well-fitted by rapid absorption of the blackbody, and progressive covering of the extended component, as the absorber moves across the source, with a covering fraction that increases smoothly from zero to ~ 1.0 . Progressive covering shows that the Comptonized emission region is extended, consistent with it originating in the accretion disk corona. The strong unabsorbed component in the dip spectra is well-modelled as the uncovered part of the Comptonized emission at all stages of dipping. There is no detectable change in the low energy cut-off of the spectrum in dipping which supports the identification of the unabsorbed part of the spectrum with the uncovered part of the ADC emission. The absorbed part of the ADC emission is rapidly removed from the 0.1–2.0 keV band of the *PSPC*, which therefore selects only the uncovered part of the emission, and so the spectral evolution in dipping as viewed by the *PSPC* depends only on the covering fraction, determined by the geometric overlap between the source and absorber.

Key words: X rays: stars – stars: individual: XB 1916-053 – stars: neutron – binaries: close – accretion: accretion disks

1 INTRODUCTION

XB 1916-053 is a member of the class of Low Mass X-ray Binary (LMXB) sources which exhibit dips in X-ray intensity at the orbital period. It is generally accepted that dipping is caused by absorption in the bulge in the outer accretion disk where the accretion flow from the companion star impacts (White & Swank 1982). XB 1916–053 has the shortest period of all dipping sources of 50 min, and is also remarkable in having a difference of $\sim 1\%$ between the X-ray and optical periods (Grindlay et al. 1988). Dipping is often very deep in this source, with the depth of dipping reaching $\sim 100\%$ in the band 1–10 keV. The source has been observed using several X-ray observatories, notably *Exosat*, *Ginga*, *ASCA* and *Rosat*. Spectral analysis of the three *Exosat* observations (Smale et al. 1988) showed that in dipping, part of the emission was clearly not absorbed. The non-dip emission was well fitted by a simple power law model. However, the dip spectra clearly contained two components: one absorbed and

the other not absorbed. These were modelled by dividing the non-dip model into two parts each having the same form as the non-dip spectrum, one absorbed, and the other not absorbed, but with a normalization that decreased strongly in dipping. This approach may be called the “absorbed plus unabsorbed” approach, and has also been used in fitting the spectra of the dip sources XB 1254-690 (Courvoisier et al. 1986) and XBT 0748-676 (Parmar et al. 1986). More recently *Ginga* data on XB 1916–053 has also been fitted by this approach (Smale et al. 1992; Yoshida et al. 1995). The parameters of the emission regions cannot, of course, change during dip intervals, and so the decrease in normalization of the unabsorbed component cannot represent a decrease in brightness of the source, and a difficulty in using “absorbed plus unabsorbed” modelling has been in finding a physical explanation for the decrease. A possible explanation for this effect which has sometimes been given is electron scattering in the absorbing region, which would reduce the X-ray flux

in an energy-independent way. In the case of XBT 0748-676, Parmar et al. (1986) suggested that the unabsorbed component was the result of rapid changes in column density which can mimic a soft excess. A further problem in absorbed plus unabsorbed modelling is in explaining the variation of the normalization of the absorbed component during dip intervals, which although approximately constant, always exhibits a wave (in the plot of normalization *versus* intensity) that is difficult to explain.

The dipping LMXB sources do not, in general, exhibit the spectral evolution in dipping expected for absorption of a single-component spectrum by cool material, ie a hardening of the spectrum, and individual sources can display hardening, energy-independence or even softening, as in X 1624-490 (Church & Bałucińska-Church, 1995). It has been possible to explain the complexity of this behaviour using the two-component model proposed by Church & Bałucińska-Church (1995), in which X-ray emission originates as point-source blackbody emission on the surface of the neutron star, or in the boundary layer at the surface, plus extended Comptonized emission, probably from the accretion disk corona (ADC). Using this model, good fits were obtained to the *Exosat* data in the case of X 1755-338, for example, in which dipping appears to be mostly due to absorption of the point-source blackbody component (Church & Bałucińska-Church 1993), and rapid variability in dipping is due to the point-like nature of this component. However in this source, dipping is less than 20% deep in the 1–10 keV band, and the implication is that the projected size of the absorbing region is smaller than the projected size of the Comptonizing region.

XB 1916–053 was observed using *ASCA* on 1993, May 2nd. Dipping was very deep, reaching 100% during every dip, showing that all emission regions became covered by absorber, and there was clear evidence for an unabsorbed part of the spectrum during dipping (Church et al. 1997). The dip spectra could be well fitted by the two-component model by allowing progressive covering of the extended Comptonized emission, and the model flux I can be expressed in the form:

$$I = e^{-\sigma N_H} \{ I_{BB} e^{-\sigma N_H^{BB}} + I_{PL} (f e^{-\sigma N_H^{PL}} + (1-f)) \} \quad (1)$$

where I_{BB} and I_{PL} are the energy-dependent fluxes of the blackbody and cut-off power law components, N_H^{BB} and N_H^{PL} are the column densities of each component during dipping, additional to the non-dip column density N_H , and σ is the photoelectric absorption cross section of Morrison and McCammon (1983). A power law is used to approximate Comptonization at energies well below the break energy. This fitting showed that the point-like blackbody is absorbed as soon as the absorber overlaps the neutron star, but the extended component is covered progressively as dipping develops as shown by the smooth increase of the covering fraction f from zero to ~ 1.0 . This is consistent with a dense absorber moving across an extended emission region, and differs from partial covering of the source regions by a “blobby” absorber having density variations such that different parts of the absorber are more or less absorbing to X-rays. Although progressive covering and partial covering by a blobby absorber are very different, both models can be represented by the same spectral model which takes no account of the geometry of overlap of source and absorber, but only of the total covering fraction.

Progressive Covering also differs substantially from the “absorbed plus unabsorbed” approach previously used for fitting the group of sources with an unabsorbed spectral component in dipping. Firstly, there is no decrease in normalization of any component and so no difficulty in explaining either the decreasing normalization of the unabsorbed component, or the wave in the normalization of the absorbed component as a function of intensity as dipping develops. Secondly, there is a clear explanation of the unabsorbed component which is simply the uncovered part of the extended Comptonized emission. In absorbed plus unabsorbed modelling, the origin of the unabsorbed component was not clear, but it was often suggested that electron scattering was responsible, clearly a radically different explanation. In fitting the *ASCA* data on XB 1916–053 (Church et al. 1997), dipping was explained purely in terms of photoelectric absorption by material with Solar abundances without requiring electron scattering in the energy band ~ 1 –10 keV, and it was shown from the Thomson and photoelectric absorption cross sections that absorption strongly dominates over electron scattering below 10 keV so that little electron scattering is, in fact, expected. With the same model, it has recently been possible to fit the spectral evolution in dipping in XBT 0748-676 during the *ASCA* PV phase observation (Church et al. 1998a). The fitting required a line feature at ~ 0.65 keV having the same progressive covering factor as the extended Comptonized emission, and as the line probably originates in the ADC, this provides strong evidence that the extended continuum emission region is also the ADC.

High quality data were also obtained on XB 1916-053 with *Rosat*, and we present here spectral analysis results in which we test whether the approach applied with the *ASCA* data can also describe dipping at lower energies in the 0.1–2.0 keV band of the *PSPC* instrument.

2 RESULTS

XB 1916-053 was observed using *Rosat* for 49 hr starting on 1992, Oct 17, corresponding to about 60 orbital cycles. Data were extracted by selection in a $2'$ radius circle centered on the source from the sky image. Background data were selected from an annular region of the image excluding all apparent point sources. The quality of background subtraction was tested by performing spectral fitting with this background data, and without subtraction, and it was found that there was little effect on spectral fitting results even if no subtraction was made.

2.1 Light Curves and Folding Analysis

The background-subtracted light curve of the observation is shown in Fig. 1 in the energy band 0.1–2.0 keV, in which one burst is evident. The data are very fragmented, and coverage of dipping is not very good, however, in 3 orbits, there is complete coverage of the dips. Period searching was carried out using a standard program which folds the data on trial periods, and provides the most likely period from the turning-point of a χ^2 *versus* period plot. In principle, the result may be further refined by producing a model template for one X-ray cycle which can be fitted sequentially to each

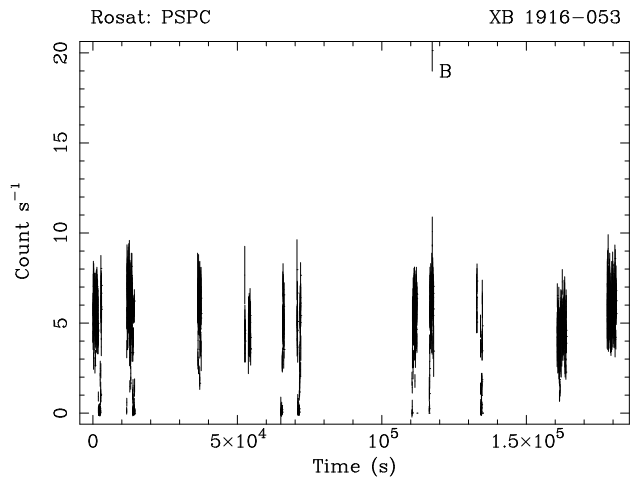


Figure 1. Light curve for the total observation in the band 0.1–2.0 keV in 16 s bins. The burst is labelled B.

cycle of the data to test whether a time difference accumulates between data and model. This method also provides error estimates for the X-ray period. In the present observation in which the coverage of dipping is not good, this is not justified, and we quote an approximate period uncertainty from the uncertainty in the peak of the χ^2 - period plot due to the errors in individual χ^2 values. The best fit X-ray period found by period searching of the complete observation in the band 0.1–2.0 keV was 3004 ± 12 s. The period uncertainty may actually be larger than quoted as all methods of error determination assume that the shape of dips does not change. The value obtained is consistent with the previous determinations: 3015 ± 17 s (Smale et al. 1986), 3005 ± 6.6 s (Smale et al. 1992) and 3005 ± 20 s (Church et al. 1997). To show the folded light curve, only the 3 orbits with good coverage of dipping were included, since if all of the data is included, dipping in the folded light curve is not 100% deep due to averaging of dips that have some differences in phase and shape, and does not reflect dipping in a typical dip.

Folded light curves in the two energy bands 0.1–1.0 keV and 1.0–2.0 keV are shown in Fig. 2. It can be seen that dipping is essentially 100% deep in both bands, and that the intensity remains close to zero during almost all of the dip until dip egress begins. This contrasts with dipping in the 1–10 keV band as revealed by *ASCA*, in which the intensity falls rapidly to $\sim 10\%$ of the non-dip level, but then more slowly, so that the intensity touches zero for only a short time at the deepest part of the dip (Church et al. 1997). This suggests that only at the deepest point in each dip is there complete overlap between the high density central regions of the absorber and the source. In the *Rosat PSPC* band, a smaller column density will lead to zero intensity and so there will be an extended period of deep dipping. Moreover, the lack of variation between the depth of dipping in the two *Rosat* energy bands is consistent with a high column density in the absorber, as was the case during the *ASCA* observation. When the hardness ratio formed from the two folded light curves is examined, there is little change in hardness ratio from the non-dip value at dip ingress or egress. In *ASCA*, there was an increase in hardness defined in terms of the bands 2.0–12.0 keV and 0.5–2.0 keV during dip ingress and egress, as dipping was not 100% in the dip transitions,

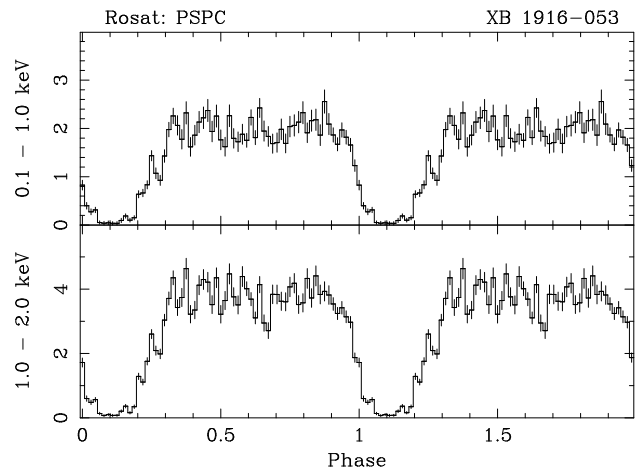


Figure 2. Light curves in the bands 0.1–1.0 keV and 1.0–2.0 keV folded on the period of 3004 s.

and not equal in these bands (Church et al. 1997). Finally, it can be seen that there appears to be asymmetry between dip ingress and egress; however this must be treated with caution because of the limited amount of dip data included in the folding.

2.2 Spectral Evolution in Dipping

The good quality of the *Rosat* data has allowed detailed spectral analysis to be carried out for non-dip data and for dip data selected in several intensity bands. Non-dip data was selected from the complete observation, but excluding the burst, from the intensity band 5.5–7.0 count s^{-1} , and 4 intensity bands: 4.0–5.5, 2.5–4.0, 1.0–2.5 and 0.0–1.0 count s^{-1} were used for dipping. Background was subtracted, systematic errors of 2% were added and the spectra regrouped appropriately, to a minimum of 100 counts per channel for the non-dip spectrum, and to minima of 80, 60, 40 and 40 counts for the 4 dip spectra (with decreasing intensity). The solar abundances of Anders and Grevesse (1989) were used throughout. Firstly, simple one-component spectral models were tried such as an absorbed power law, absorbed bremsstrahlung and absorbed blackbody models. In all model fitting, the emission parameters were fixed in fitting dip spectra at the non-dip values, since dipping is due to absorption, not source changes; thus for the simple blackbody model the blackbody temperature and normalisation were fixed. This model gave a marginally unacceptable fit to the non-dip spectrum, whereas the bremsstrahlung model gave an acceptable fit. However, both models were quite unable to fit dip data, giving reduced χ^2 values of 3.98 and 3.25 respectively for a simultaneous fit to non-dip and 4 dip levels. The power law model gave a good fit to the non-dip data, but was also unable to fit dip spectra because of strong excesses at low energies of the model over the data. Thus dipping cannot be modelled by simple absorbed models, and it was clear that an ‘unabsorbed component’ was present, ie part of the non-dip emission persisted at low energies in dipping and was not absorbed. We next tried the two-component model with progressive covering of the extended emission which gave a good fit to the *ASCA* data, represented by equation 1. The point-like blackbody is as-

sumed to be covered immediately the absorber overlaps the emission region, ie the neutron star.

The *ASCA* results (Church et al. 1997) showed that the blackbody component had $kT_{\text{BB}} = 2.1$ keV, peaking outside the *Rosat* band and so the flux of this component in the 0.1-2.0 keV band is expected to be small, assuming the source did not change markedly between the observations, making it difficult to determine blackbody parameters. Consequently, we first tried the above model omitting the blackbody, and then repeated the fitting with the blackbody added. The results for the power law component did not change markedly, and sensible values for blackbody parameters were obtained. In this case, it is clearly better to present results from the fitting with the blackbody present than with it omitted, or with blackbody parameters set to the *ASCA* values.

Firstly, simultaneous fitting was carried out to the non-dip spectrum and all dip levels, and good fits were obtained. Best fit values of $kT_{\text{BB}} = 1.95^{+0.74}_{-0.34}$ keV, and power law photon index $\Gamma = 2.32 \pm 0.04$ were obtained, and the column density for the non-dip spectrum = $3.9 \pm 0.1 \times 10^{21}$ H atom cm^{-2} . Very similar values were obtained by fitting the non-dip spectrum alone. Although Γ appears to be well-determined, the band of the *PSPC* is relatively narrow for determining power law index values (see Sect. 3).

Parameters for the 4 dip spectra were further optimized by fitting these individually keeping kT_{BB} , Γ and the normalizations at the best-fit values. The results are shown in Fig. 3 and Table 1, which gives the blackbody and power law column densities N_{H}^{BB} and N_{H}^{PL} during dipping *additional* to the non-dip column density, and the progressive covering fraction f . The column densities and the covering fraction f are plotted a function of X-ray intensity in the band 0.1–2.0 keV at different stages of dipping in Fig. 4. These results show that during dipping, the power law emission is progressively covered until in the deepest dip spectrum, f is 97% and the power law column density has risen to $>10^{23}$ H atom cm^{-2} . However, the covered part of the power law emission is quickly removed to energies greater than 2 keV, and we have the interesting situation that the *PSPC* effectively only detects and measures the properties of the uncovered, ie the unabsorbed part of the spectrum. The blackbody suffers relatively little absorption until the partial covering fraction is $\sim 50\%$, at which point it increases rapidly, and by the second level of dipping (in the band 2.5–4.0 count s^{-1} , the blackbody flux in the *PSPC* is close to zero, and for the remaining levels of dipping, it is zero. The larger values of N_{H} for the blackbody are expected since this point source emission effectively monitors regions towards the centre of the absorber, whereas the extended Comptonized emission gives an N_{H} integrated across the absorber. The lack of change in column density for the blackbody until f becomes appreciable might also be expected in terms of our physical picture of an extended absorber which would have to cover part of the ADC before reaching the neutron star.

Although the *PSPC* is not ideally suited to determining values of Γ , it is ideal for investigating the spectrum in the region of the low energy cut-off, and comparison of the non-dip and dip spectra shown in Fig. 3 reveals that there is no detectable change in the low energy cut-off, which is strong evidence that the unabsorbed part of the spectrum is the uncovered part of the non-dip emission.

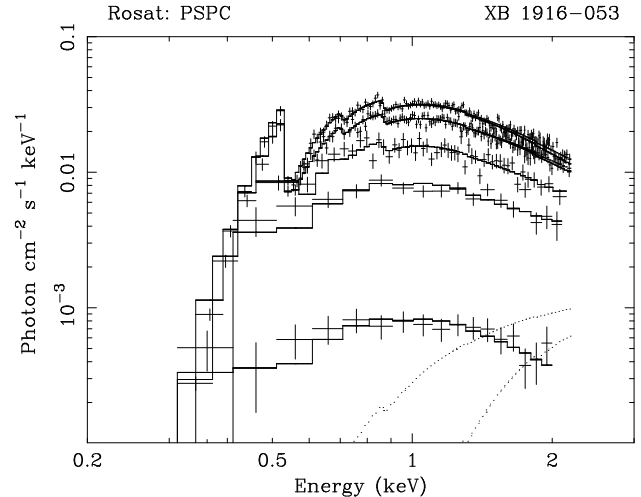


Figure 3. Spectral fitting results for non-dip and 4 levels of dipping. The total model is shown as a stepped line, and the blackbody contribution (only visible for the non-dip and first level of dipping) is shown dotted.

Table 1. Best fit spectral fitting results. Intensities I are in count s^{-1} , and N_{H} values are column densities additional to non-dip values and are in units of 10^{22} H atom cm^{-2} .

I	N_{H}^{BB}	N_{H}^{PL}	f	χ^2/dof
5.5 - 7.0	0.0	0.0	0.0	154/165
4.0 - 5.5	$1.4^{+2.9}_{-0.9}$	$2.5^{+1.0}_{-0.5}$	0.208 ± 0.020	146/153
2.5 - 4.0	>20	4.2 ± 1.8	0.503 ± 0.014	53/47
1.0 - 2.5	>20	5.0 ± 1.6	0.736 ± 0.013	24/18
0.0 - 1.0	>20	>20	0.974 ± 0.003	13/18

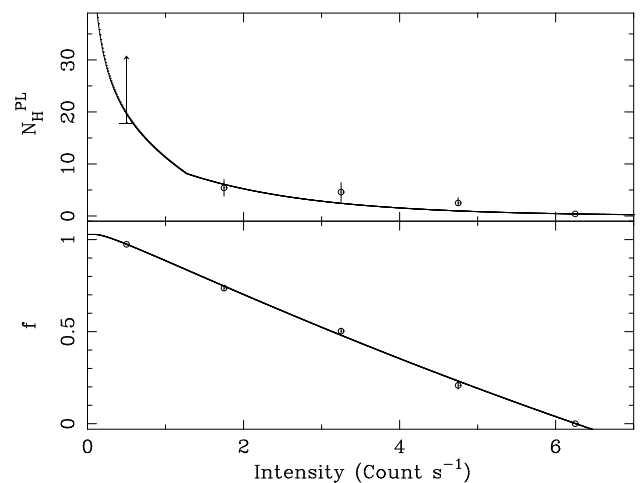


Figure 4. The covering fraction f and column density N_{H}^{PL} in units of 10^{22} H atom cm^{-2} of the extended power law emission component as a function of source intensity. The solid lines show polynomial fits to the data points.

3 DISCUSSION

The LMXB source XB 1916–053 was observed with *Rosat*, and during this observation dipping was 100% deep at all energies in the *PSPC* band, showing that all emission regions were completely covered by the absorbing region. The *PSPC* spectra are well fitted by the two-component model proposed by Church and Bałucińska-Church (1995) consisting of point-like blackbody emission from the surface or boundary layer at the surface of the neutron star, plus extended Comptonized emission from the ADC. Good fits to the dip spectra are obtained by allowing progressive covering of the extended emission component, with the covering fraction rising smoothly from zero to close to unity. This, together with the large values of column density determined for the dip spectra, demonstrates that the absorber is large and dense, and moves progressively across the extended source region. Thus the covering is not partial in the sense of a “blobby” absorber, ie an absorber partially transmitting to X-rays between high density regions. The blackbody emission, on the other hand, is very rapidly absorbed once the absorber covers the neutron star. The high quality *PSPC* spectra show clearly that there is no detectable change in the low energy cut-off of the spectrum from non-dip to any of the stages of dipping, strongly supporting the contention that the unabsorbed emission is simply the uncovered part of the extended ADC emission. This approach differs radically from the “absorbed + unabsorbed” modelling, often used previously for this source and similar sources in which the nature of the unabsorbed peak, or soft excess, was seen as being due to electron scattering or possibly fast changes of column density mimicing a soft excess. In the progressive covering model, there is a simple explanation of the unabsorbed component as uncovered emission. The progressive covering model also differs in its application, since the normalizations of the spectral components are fixed, and the difficulty in explaining the changing normalizations in absorbed plus unabsorbed modelling does not exist. With the progressive covering model, it is not necessary to invoke an explanation for the unabsorbed component such as being due to electron scattering, and dipping is explained entirely in terms of photoelectric absorption. We do not need to invoke electron scattering in fitting either the *Rosat* or the *ASCA* data, and calculations of the relative loss of X-ray intensity by the two processes: electron scattering and photoelectric absorption show that absorption strongly dominates at most energies below 10 keV. However above 10 keV, the Thomson cross section becomes larger than that for photoelectric absorption and dipping above 10 keV may involve a degree of electron scattering.

From the results shown in Table 1, the covering fractions f may be used to calculate the relative energy fluxes of the absorbed and unabsorbed parts of the spectrum, ie the covered and uncovered components. In the band 0.1–2.0 keV, the percentage of the absorbed part was found to have the values: 0%, 2.6%, 3.2%, 5.6% and 0.1% for the sequence of 5 spectra going from non-dip to deep dipping. As the source progresses into dipping, the effective normalization of the absorbed power law component (f times the actual normalization) increases as f increases. N_{H} also increases, and so the percentage of this component peaks at about 6%. Consequently, the *PSPC* acts as a very good filter in allowing

measurement of the unabsorbed part, essentially alone. The main consequence of this is that the most important parameter determining the *PSPC* spectra is f ; column densities do not affect the uncovered part of the power law emission, and hence f can be determined with good accuracy. Thus the spectral evolution in dipping is determined in the *Rosat* band by the geometric overlap between the extended source component and the absorber, and the values of f can be used in principle to determine the shape of the absorber for given assumed simple shapes of the ADC. To do this, values for f should be obtained as a function of orbital phase, not intensity. However, allowing for the need for a minimum of 7 phase bins to cover non-dip, ingress, deep dip and egress, the quality of the present data do not allow us, for example, to discriminate between geometric models for the ADC.

The power law index was found to have a value of 2.3, however it should be borne in mind that the band of energies available in the *PSPC* from which an index can be obtained is very narrow. Recent work on the source using the very broad band of *BeppoSAX* of 0.1–300 keV (Church et al. 1998b) has shown that the non-dip spectrum is well fitted by a blackbody plus cut-off power law model, with a cut-off energy of ~ 80 keV. The underlying power law photon index may, of course, be well determined using this very wide band, and it was shown that with more restricted energy bands, there is a tendency to overestimate values of the index. Using the LECS and MECS bands without the other instruments, ie in the energy range 0.1–10 keV, $\Gamma \sim 1.75$ whereas in the total band extending to >100 keV, $\Gamma \sim 1.6$. A similar effect, or larger, may be expected in the present work. However, it is clear that the progressive covering model gives a good explanation of spectral evolution in dipping in XB 1916-053, and has also been shown to describe dipping well in XBT 0748-676 (Church et al. 1998a), and it represents an improvement in our understanding of these sources. An interesting question that remains is why do some sources such as XB 1916-053 and XBT 0748-676 have the extended emission component often totally absorbed, whereas in others, for example, X 1755-338, there is apparently little absorption of this emission.

REFERENCES

- Anders E., and Grevesse N., 1989, *Geochimica et Cosmochimica Acta* 53, 197.
- Church M. J. and Bałucińska-Church M., 1993, *MNRAS* 260, 59.
- Church M. J. and Bałucińska-Church M., 1995, *A&A* 300, 441.
- Church M. J., Dotani T., Bałucińska-Church M., Mitsuda K., Takahashi T., Inoue H. and Yoshida K., 1997, *ApJ*, 491, 388.
- Church M. J., Bałucińska-Church M., Dotani T. and Asai K., 1998a, *ApJ In Press*
- Church M. J., Parmar A. N., Bałucińska-Church M., Oosterbroek T. and Dal Fiume D., *A&A*, 1998b *In Press*.
- Courvoisier T. J.-L., Parmar A. N., Peacock A. and Pakull M., 1986, *ApJ* 309, 265.
- Grindlay J. E., Bailyn C. D., Cohn H., Lugger P. M., Thorstensen J. R. and Wegner G., 1988, *ApJ* 334, L25
- Morrison R., and McCammon D., 1983, *ApJ* 270, 119.
- Parmar A. N., White N. E., Giommi P. and Gottwald M., 1986, *ApJ* 308, 199.
- Smale A. P., Mason K. O., White N. E. and Gottwald M., 1988, *MNRAS* 232, 647.

Smale A. P., Mukai K., Williams O. R., Jones M. H. and Corbet
R. H. D., 1992, ApJ 400, 330.
White N. E. and Swank J. H., 1982, ApJ 253, L66.
Yoshida K., Inoue H., Mitsuda K., Dotani T. and Makino F.,
1995, PASJ 47, 141.